7-9-2012

Near field enhancement in silver nanoantenna-superlens systems

Zhengtong Liu
Inst High Performance Comp

Erping Li
Inst High Performance Comp

Vladimir M. Shalaev
Birck Nanotechnology Center, Purdue University, shalaev@purdue.edu

Alexander V. Kildishev
Birck Nanotechnology Center, Purdue University, kildishev@purdue.edu

Follow this and additional works at: http://docs.lib.purdue.edu/nanopub

Part of the Nanoscience and Nanotechnology Commons

Near field enhancement in silver nanoantenna-superlens systems

Zhengtong Liu, Erping Li, Vladimir M. Shalaev, and Alexander V. Kildishev

Additional information on Appl. Phys. Lett.

Near field enhancement in silver nanoantenna-superlens systems

Zhengtong Liu (刘政通),[1,a] Erping Li (李尔平),[1] Vladimir M. Shalaev,[2]
and Alexander V. Kildishev[2]

[1]*Department of Electronics & Photonics, Institute of High Performance Computing, 1 Fusionopolis Way,
#16-16 Connexis North, Singapore 138632*
[2]*School of Electrical and Computer Engineering and Birck Nanotechnology Center, Purdue University,
West Lafayette, Indiana 47907, USA*

We demonstrate near field enhancement generation in silver nanoantenna-superlens systems via numerical modeling. Using near-field interference and global optimization algorithms, we can design nanoantenna-superlens systems with mismatched permittivities, whose performance can match those with matched permittivities. The systems studied here may find broad applications in the fields of sensing, such as field-enhanced fluorescence and surface-enhanced Raman scattering, and the methodology used here can be applied to the designing and optimization of other devices, such as two-dimensional near field focusing lens. © 2012 American Institute of Physics. [http://dx.doi.org/10.1063/1.4732793]

Plasmonic nanoantennas and superlens have attracted great attention recently due to their potential applications in biosensing (including including surface enhanced Raman scattering (SERS) and surface enhanced fluorescence), photolithography, quantum optical information processing, and other technologies.[1–7] A plasmonic nanoantenna is usually made of paired metal nanoparticles under resonance conditions, and it is capable of generating "hot spots" with a highly localized and significantly enhanced electromagnetic field.[8–15] These hot spots have many applications, especially for biomedical sensing such as SERS (Ref. 16) and surface enhanced fluorescence.[17–22] A perfect lens is a planar material slab with simultaneously negative permittivity and permeability which can focus propagating waves and enhance evanescent waves, thereby does not suffer from the diffraction limit.[7] When the source object is in the near field of the slab, the electrostatic approximation is valid and the requirement can be relaxed to $\varepsilon_1 = -\varepsilon_2$, where ε_1 and ε_2 are the permittivities of the slab and the host material, respectively. This condition can be readily satisfied by metals such as gold and silver at optical frequencies. Such a thin metal slab is often referred to as a near-field superlens.[7,23]

In one of our previous works, we combined the nanoantenna and superlens concepts to create a sensing device-a nanoantenna-superlens system.[24] We have shown that if we place a nanoantenna close to a near-field superlens, the hot spot generated by the nanoantenna can be translated to the other side of the superlens. By doing so, we can avoid the undesirable fluorescence quenching or structural (denaturation) and/or functional changes of molecules in biochemical sensing caused by the close contact of metal surfaces and the molecules, while still benefit from local field enhancement provided by nanoantennas.[25–29] However to satisfy the operational condition of superlens, we had to use a metal-dielectric composite superlens to match the permittivity of the host material. While using composite for superlens provides certain degree of tunability, the effective permittivity

of a metal-dielectric composite depends on many fabrication conditions and is difficult to control, and the effective medium theory does not take into account many factors, such as particle size and annealing temperature, therefore may not accurately describe the optical properties of the composite. This uncertainty significantly limits the actual application of the nanoantenna-superlens system.

Recently, we have studied the coupling effect in a near-field object-superlens system.[30] We have found out that the coupling effect between the object and the superlens significantly alters the field distribution around both the object and the superlens and creates complex near-field interference patterns. By using the coupling effect, it is possible to design a nanoantenna-superlens system to translate hot-spots with mismatched permittivities, eliminating the need for composite materials. In this report, we present such nanoantenna-superlens systems made of pure silver and show that they can achieve similar performance compared to the previous systems made of composites.[24]

The side view and top view of a unit cell of the nanoantenna-superlens system we studied are shown in Fig. 1. Each unit cell consists of a nanoantenna and a slab of superlens. The nanoantenna is composed of two closely spaced elliptical silver cylinders embedded in a dielectric host, and the superlens is a uniform silver slab placed above the nanoantenna with a thin dielectric spacer between the nanoantenna and the superlens. Above the silver superlens is a thin dielectric cover layer that protects the superlens and separates the superlens from molecules under detection. All dielectric is SiO_2, and the incoming light is a plane wave normally incident from bottom with a wavelength of 633 nm. The wavelength is chosen because it is a most common laser wavelength and in real applications can be set to any wavelength of interests. At this wavelength, the permittivity of silver is $-17.9 + 0.477i$, and the permittivity of SiO_2 is 2.12, obviously they mismatch and do not satisfy the operational condition of superlens, which requires that $\varepsilon_1 = -\varepsilon_2$, where ε_1 and ε_2 are the permittivities of the superlens and the host dielectric, respectively. In our discussions that follow, the
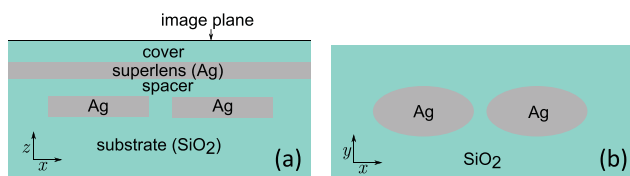
a)Email: liuzt@ieee.org.

FIG. 1. (a) Side view of a unit cell and (b) Top view of a unit cell.

superlens interface closer to the nanoantenna is referred to as the bottom interface, while the other side is the top interface.

Nanoantenna arrays have been studied experimentally and numerically in our previous work, where it has been shown that the arrays can be accurately modeled using the finite element method (FEM).[31] The nanoantenna-superlens system was numerically modeled and optimized using a commercial FEM software package COMSOL MULTIPHYSICS. The thickness of the silver superlens was set to 20 nm, with which a uniform silver film can be deposited. The gap width of the nanoantenna was set to 20 nm, which can be reliably fabricated using electron beam lithography. The thickness of the cover layer was set to 10 nm. The other dimensions in the system were optimized using global optimization algorithms to achieve highest electric field enhancement at the center of the image plane, which was a plane 1 nm above the cover layer where molecules under sensing will be placed.

The optimized dimensions were period along x axis 680 nm, period along y axis 328 nm, ellipse major axis 208 nm, ellipse minor axis 92 nm, antenna thickness 43 nm, and spacer thickness 14 nm. The electric field intensity enhancement (EFIE) maps are plotted in Fig. 2. Fig. 2(a) shows the EFIE at the image plane, and the blue ellipses are the outline of the nanoantenna. The translated hot spot is clearly shown, with the EFIE up to 50. The EFIE map inside the nanoantenna gap is plotted in Fig. 2(b) for comparison, and the inset of Fig. 2(b) shows the gap region magnified. Comparing Figs. 2(a) and 2(b), it is clear that the hot spot in the nanoantenna gap is translated to the other side of superlens with reduced magnitude and increased size. Although the magnitude of the translated field enhancement is not as high as that inside the antenna gap, the volume of the translated hot spot is much larger than the nanoantenna gap, which is beneficial for molecular detection techniques such as surface-enhanced Raman scattering. The EFIE in the nanoantenna gap without the silver superlens (silver is

replaced by quartz) is plotted in Fig. 2(c) for reference, and it is clear that EFIE is reduced compared to Fig. 2(b). The silver superlens not only translates the hot spot but also alters the field on the nanoatenna side.

Since the field enhancement in the nanoantenna-superlens system is caused by near field interference, it is possible that the hot spots are not at the center of the unit cells. If we relax the constraints and optimize the highest field in the whole image plane, we can achieve even higher field enhancement. Using this criterion, one set of the optimized dimensions was period along x axis 1173 nm, period along y axis 350 nm, ellipse major axis 265 nm, ellipse minor axis 206 nm, antenna thickness 45 nm, and spacer thickness 34 nm. Other dimensions remained unchanged (20 nm gap, 20 nm superlens, and 10 nm cover). The EFIE map of two unit cells at the image plane with this configuration is plotted in Fig. 3(a). The highest EFIE in this case is above 250, much higher than that in Fig. 2(a). The field pattern is also drastically different, with hot spots not at the center of the unit cells but at the edges. Fig. 3(b) shows the EFIE inside the nanoantenna gaps. It is obvious that the highest EFIE locations at the image plane are not directly above the gaps, while the hot spots on the nanoantenna side are clearly inside the gaps. This illustrates that our system is not a simple near-field imaging system but rather a complex coupled near-field interference system. The EFIE in the nanoantenna gaps without the silver superlens (Fig. 3(c)) is drastically lower than that in Fig. 3(b) with the superlens, which suggests strong coupling between the superlens and the nanoantennas.

We have demonstrated near field enhancement generation in silver nanoantenna-superlens systems through numerical modeling. Depending on the optimization criteria, the highest electric field intensity enhancement may go up to 50 or 250. Although the systems we have studied here are very similar to those in our previous work,[24] their operational principles are not exactly the same. Here, we used slabs made of pure silver instead of metal-dielectric composite and host material SiO_2 instead of Si. Their permittivities do not match to satisfy the superlens working condition ($\varepsilon_1 = -\varepsilon_2$) at the operational wavelength of choice. Therefore, the field enhancement at the image plane is not a simple translation of the hot spots inside the nanoantenna gaps, but rather a result of near field interference. Near field interference has also been explored for other applications, for example hypergratings and near field focusing lens.[32,33] In this
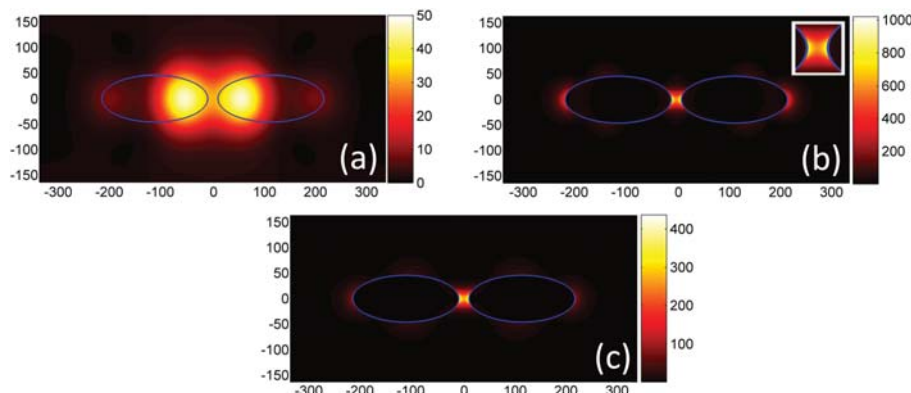

FIG. 2. (a) The electric field intensity enhancement (EFIE) at the image plane; (b) the EFIE inside the nanoantenna gap; and (c) the EFIE inside the nanoantenna gap without the silver superlens. The unit of dimensions is nm.
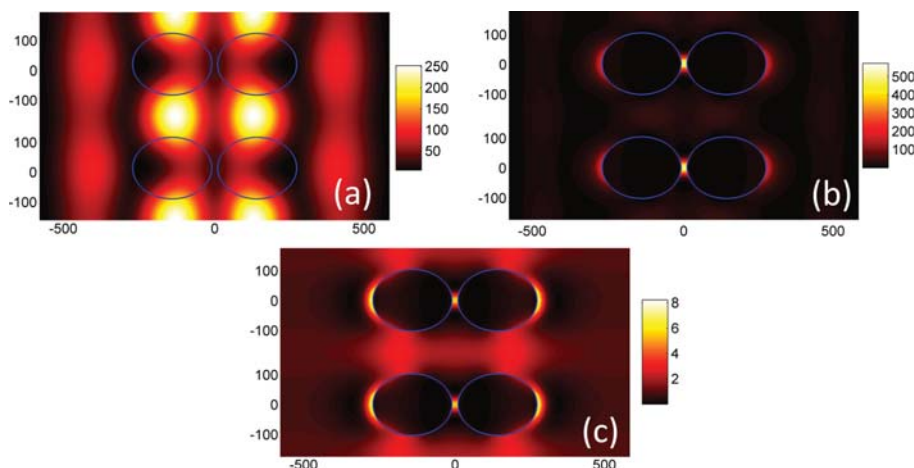
FIG. 3. (a) The EFIE at the image plane; (b) the EFIE inside the nanoantenna gaps; and (c) the EFIE inside the nanoantenna gaps without the silver superlens. Two unit cells are shown in the plots to show the hot spots clearly. The unit of dimensions is nm.

work, we have chosen a wavelength of 633 nm to demonstrate the nanoantenna-superlens systems, simply because this is a commonly used wavelength and light sources at this wavelength are readily available. For real life applications, the working wavelength may be set arbitrarily according to the actual needs. Using optimization algorithms to optimize near field interference patterns, we can design nanoantenna-superlens systems with a broad variety of materials and shapes, which greatly expands the scope of applications of our nanoantenna-superlens systems.

[1]P. Muhlschlegel, H. J. Eisler, O. J. F. Martin, B. Hecht, and D. W. Pohl, Science **308**, 1607 (2005).
[2]W. Rechberger, A. Hohenau, A. Leitner, J. R. Krenn, B. Lamprecht, and F. R. Aussenegg, Opt. Commun. **220**, 137 (2003).
[3]J. N. Farahani, D. W. Pohl, H.-J. Eisler, and B. Hecht, Phys. Rev. Lett. **95**, 017402 (2005).
[4]J. N. Farahani, H.-J. Eisler, D. W. Pohl, M. Pavius, P. Flückiger, P. Gasser, and B. Hecht, Nanotechnology **18**, 125506 (2007).
[5]E. Cubukcu, E. A. Kort, K. B. Crozier, and F. Capasso, Appl. Phys. Lett. **89**, 093120 (2006).
[6]A. Sundaramurthy, P. J. Schuck, N. R. Conley, D. P. Fromm, G. S. Kino, and W. E. Moerner, Nano Lett. **6**, 355 (2006).
[7]J. B. Pendry, Phys. Rev. Lett. **85**, 3966 (2000).
[8]P. K. Aravinda, A. Nitzanb, and H. Metiu, Surf. Sci. **110**, 189 (1981).
[9]E. Hao and G. C. Schatz, J. Chem. Phys. **120**, 357 (2004).
[10]R. M. Bakker, A. Boltasseva, Z. Liu, R. H. Pedersen, S. Gresillon, A. V. Kildishev, V. P. Drachev, and V. M. Shalaev, Opt. Express **15**, 13682 (2007).
[11]V. M. Shalaev, M. I. Shtockman, Sov. Phys. JETP **65**, 287 (1987).
[12]V. A. Markel, L. S. Muratov, M. I. Stockman, and T. F. George, Phys. Rev. B **43**, 8183 (1991).
[13]M. I. Stockman, L. N. Pandey, L. S. Muratov, and T. F. George, Phys. Rev. Lett. **72**, 2486 (1994).
[14]D. P. Tsai, J. Kovacs, Z. Wang, M. Moskovits, V. M. Shalaev, J. S. Suh, and R. Botet, Phys. Rev. Lett. **72**, 4149 (1994).
[15]V. M. Shalaev, Phys. Rep. **272**, 61 (1996).
[16]*Surface-Enhanced Raman Scattering*, edited by K. Kneipp, M. Moskovits, and H. Kneipp (Springer, Berlin, 2006).
[17]V. Giannini and J. A. Sánchez-Gil, Opt. Lett. **33**, 899 (2008)
[18]S. Kühn, G. Mori, M. Agio, and V. Sandoghdar, Mol. Phys. **106**, 893 (2008).
[19]R. M. Bakker, H.-K. Yuan, Z. Liu, V. P. Drachev, A. V. Kildishev, and V. M. Shalaev, Appl. Phys. Lett. **92**, 043101 (2008).
[20]T. H. Taminiau, R. J. Moerland, F. B. Segerink, L. Kuipers, and N. F. van Hulst, Nano Lett. **7**, 28 (2007).
[21]F. Jäckel, A. A. Kinkhabwala and W. E. Moerner, Chem. Phys. Lett. **446**, 339 (2007).
[22]R. M Bakker, V. P Drachev, Z. Liu, H.-K. Yuan, R. H. Pedersen, A. Boltasseva, J. Chen, J. Irudayaraj, A. V. Kildishev, and V. M Shalaev, New J. Phys. **10**, 125022 (2008).
[23]N. Fang, H. Lee, C. Sun, and X. Zhang, Science **308**, 534 (2005).
[24]Z. Liu, M. D. Thoreson, A. V. Kildishev, and V. M. Shalaev, App. Phys. Lett. **95**, 033114 (2009).
[25]P. Anger, P. Bharadwaj, and L. Novotny, Phys. Rev. Lett. **96**, 113002 (2006).
[26]J. R. Lakowicz, Anal. Biochem. **298**, 1 (2001).
[27]K. R. Brown, A. P. Fox, and M. J. J. Natan, Am. Chem. Soc. **118**, 1154 (1996).
[28]R. E. Holt and T. M. J. Cotton, Am. Chem. Soc. **111**, 2815 (1989).
[29]M. Yang, F. L. Chang, and M. Thompson, Anal. Chem. **65**, 3713 (1993).
[30]Z. Liu, V. M. Shalaev, and A. V. Kildishev, Appl. Phys. A **107**, 83 (2012).
[31]Z. Liu, A. Boltasseva, R. H. Pedersen, R. Bakker, A. V. Kildishev, V. P. Drachev, and V. M. Shalaev, Metamaterials **2**, 45 (2008).
[32]S. Ishii, A. V. Kildishev, V. M. Shalaev, K.-P. Chen, and V. P. Drachev, Opt. Lett. **36**, 451–453 (2011).
[33]X. Ni, S. Ishii, M. D. Thoreson, V. M. Shalaev, S. Han, S. Lee, and A. V. Kildishev, Opt. Express **25**, 25242–25254 (2011).